



Effect of different solvent ratio (ethylene glycol/water) on the preparation of Pt/C catalyst and its activity toward oxygen reduction reaction

Journal:	<i>RSC Advances</i>
Manuscript ID:	RA-ART-05-2015-008068.R1
Article Type:	Paper
Date Submitted by the Author:	05-Jun-2015
Complete List of Authors:	Wang, Yan-Jie; University of British Columbia, Chemical & Biological Engineering; Vancouver International Clean-Tech Research Institute, Zhao, Nana; Vancouver International Clean-Tech Research Institute, Fang, Baizeng; University of British Columbia, Department of Chemical & Biological Engineering Li, Hui; National Research Council Canada, Electrochemical Materials, Energy, Mining and Environment Wang, Haijiang; National Research Council Canada, Electrochemical Materials, Energy, Mining and Environment Bi, Xiaotao; University of British Columbia, Chemical & Biological Engineering



ARTICLE

Effect of different solvent ratio (ethylene glycol/water) on the preparation of Pt/C catalyst and its activity toward oxygen reduction reaction†

Received 00th January 20xx,
Accepted 00th January 20xx

DOI: 10.1039/x0xx00000x

www.rsc.org/

Yan-Jie Wang,^{a,b} Nana Zhao,^b Baizeng Fang,^a Hui Li,^{*c} Xiaotao T. Bi^{*a} and Haijiang Wang^{*c}

Highly dispersed 50 wt% Pt nanoparticles supported on carbon were successfully synthesized via a simple modified polyol method using different solvent volume ratios (ethylene glycol/water). The control of water proportion is found to have an important effect on the physicochemical properties of the in-house synthesized Pt/C catalysts. The structural and electrochemical characterizations reveal that the addition of water not only favors the homogeneous distribution of Pt particles with reduced particle size but also improves the electrocatalytic properties. In particular, at an optimum volume ratio of ethylene glycol to water of 45:23 among all studied ratios, the TEM images indicate that the as-synthesized Pt/C catalyst has a minimum particle size of 2.2 ± 0.5 nm, which is close to that of the commercial 46.6 wt% Pt/TKK catalyst, while the electrochemical measurements disclose electrochemical active surface areas and oxygen reduction reaction activity comparable to those of the commercial 46.6 wt% Pt/TKK catalyst. The simplicity of the synthesis process associated with the ease of filtering step due to the addition of water has significant implications for its practical application in large scale production of Pt/C catalysts for polymer electrolyte membrane fuel cells.

Introduction

Fuel cells are recognized as one of the most promising clean energy conversion technologies under development.¹⁻⁷ As one of the low temperature fuel cells, polymer electrolyte membrane (PEM) fuel cells have been demonstrated to be typical devices that can convert chemical energy of fuels such as hydrogen directly to electrical energy.⁸⁻¹⁹ Among the components of a PEM fuel cell, platinum (Pt)-based electrocatalysts play a key role in energy conversion and account for over 55% of the total stack cost because of the precious Pt as an essential element in constructing cathodic catalysts of high activity.^{20,21} Currently, the state-of-the-art and the most practical electrocatalysts for PEM fuel cells are still carbon-supported Pt catalysts because among all pure metals, Pt supported on carbon has the highest catalytic activity toward the oxygen reduction reaction (ORR).²²⁻²⁵

To improve the power density and cell voltage of an operating fuel cell at a given current density, significant efforts have been made to enhance the activity of a catalyst used in the membrane electrode assembly (MEA) that is a so-called "heart of fuel cell".²⁶ In the case of a supported Pt catalyst in a PEM fuel cell, the Pt loading of supported Pt catalysts is often fixed in the range of 20 - 40 wt%.^{25,27} Generally, the lower the Pt loading of catalyst is, the thicker the catalyst layer is at the same Pt usage on the electrode. In that case, the internal resistance of the electrode is improved while mass transport between reactants (e.g. H₂ and O₂) and products in the electrode is limited in the PEM fuel cell.²⁸⁻³⁰ Therefore, it is very important to utilize supported Pt catalysts with a high Pt loading. However, with an increasing Pt loading of catalysts above 40 wt%, the challenge of controlling the Pt particle size (<5 nm) and distribution significantly exists in the synthesis of Pt/C catalyst due to the agglomeration of nanoparticles from Pt precursors' reduction in a wet-chemistry reaction and/or carbon surface's combustion in a thermal-treatment.³¹ According to Antolini,³² when the Pt loading of catalysts was changed from 20 to 60 wt%, the size of the Pt nanoparticles increased about 4 times so that the benefit of increasing Pt loading of catalysts was not obtained under a PEM fuel cell operation.³³ So it is important to control the Pt size and distribution at high Pt loading above 40 wt%. It is reported that the selected synthesis method can determine the size and distribution of Pt that are related to physicochemical

^a Department of Chemical and Biological Engineering, University of British Columbia, 2360 East Mall, Vancouver, BC, Canada, V6T 1Z3. E-mail address: xbi@chbe.ubc.ca, Tel: 1-604-822-4408.

^b Vancouver International Clean-Tech Research Institute Inc., 4475 Wayburne Drive, Burnaby, Canada, V5G 4X4.

^c Electrochemical Materials, Energy, Mining and Environment, National Research Council Canada, 4250 Wesbrook Mall, Vancouver, BC, Canada, V6T 1W5. Email: Hui.Li@nrc-cnrc.gc.ca, Haijiang.Wang@nrc-cnrc.gc.ca. Tel: 1-604-221-3000 (Ext5592), 1-604-221-3038.

†Electronic Supplementary Information (ESI) available: XRD pattern for unsupported Pt black, CV and linear sweep voltammograms obtained before and after durability tests for Pt/C(3) and commercial Pt/TKK. See DOI: 10.1039/x0xx00000x

properties of Pt/C catalysts, in particular, the electrocatalytic properties in PEM fuel cell application.^{34,35}

In recent years, extensive efforts have been carried out to develop carbon-supported Pt catalysts by various synthesis strategies.^{23,34} As one of synthesis methods, the polyol method has been usually used in the preparation of Pt/C catalysts because of its simple experimental procedure with a solvent of ethylene glycol (EG). However, for Pt/C catalysts with a Pt loading above 40 wt%, some assist approaches are often used in the modification of polyol method to control the size of Pt nanoparticles within a narrow distribution of 1-5 nm.³³ Typically, with an assistance of pulse-microwave, Song et al.³⁶ modified a conventional polyol method to prepare the 50 wt% Pt supported on XC-72R carbon black when EG was used as solvent and reducing agent. The size of Pt nanoparticles around 2.7 nm was observed after a fast reduction process. The 50 wt% Pt/C showed a comparable ORR activity to the commercial one. In Yu's group,²³ urea was used as a special pH adjustment in a modified polyol process to prepare 60 wt% Pt/C with a Pt size of 2.2-3.3 nm because the hydrolysis of urea can generate OH⁻ gradually and thus favor the precipitation and distribution of Pt during the reduction process. Also, instead of heating method, the same group utilized γ -irradiation in the reduction of Pt precursor after the hydrolysis of urea.³⁷ The Pt size was obtained in a range of 2.3-3.4 nm for their Pt/C products. Compared with other strategies such as conventional NaBH₄ reduction and conventional polyol method, their modified polyol method resulted in better electrocatalytic performance at the Pt loading of 60 wt%.

Generally, most of modified polyol methods are very complex, time-consuming, and costly for the preparation of Pt/C catalysts with a Pt loading higher than 40 wt%. To prevent the agglomeration of Pt nanoparticles, an additive and/or stabilizing agent(s) is often used. However, the utilization of an additive introduces additional procedures in the synthesis process to remove the agent(s) which would otherwise remain in the catalyst and become a potential poisoning species of the catalyst. Therefore, it is very crucial to develop a process that uses an additive that can be relatively easily removed without adding too much additional complexity to the process. In this study, an aqueous EG mixture was used as a substitution for pure EG to prepare 50wt% Pt/C catalysts. On the one hand, the EG diluted by water can control the Pt reduction rate in the reaction and thus tune the size distribution and prevent agglomeration of Pt nanoparticles.³⁸ On the other hand, the addition of water is favourable for the removal of EG during the purification of Pt/C product because pure EG is sucked and trapped easily in the inner and outer walls of carbon pores due to its high viscosity, resulting in the difficulty to be washed out completely. The structural characterization and electrochemical measurements are carried out to examine the effect of different solvent ratios of EG/water on the structure and electrochemical properties of the 50 wt% Pt/C catalysts.

Experimental

Materials. 22.2 wt% chloroplatinic acid aqueous solution was self-prepared from chloroplatinic acid hexahydrate (H₂PtCl₆·6H₂O, ACS reagent, Sigma-Aldrich). Carbon black (Ketjen black 600J, AkzoNobel), 1M NaOH aqueous solution (Alfa Aesar), perchloric acid (HClO₄, 70 wt%, ACS reagent, Sigma-Aldrich), iso-propyl alcohol (Fisher Scientific), high-purity O₂ (99.9%, Praxair), and high-purity N₂ (99.9%, Praxair) were used as received. Water was supplied by a Millipore system (18.3 M Ω ·cm). The commercial carbon supported platinum catalyst (TEC10E50E, 46.6 wt% Pt) was purchased from Tanaka Kikinzoku Kogyo.

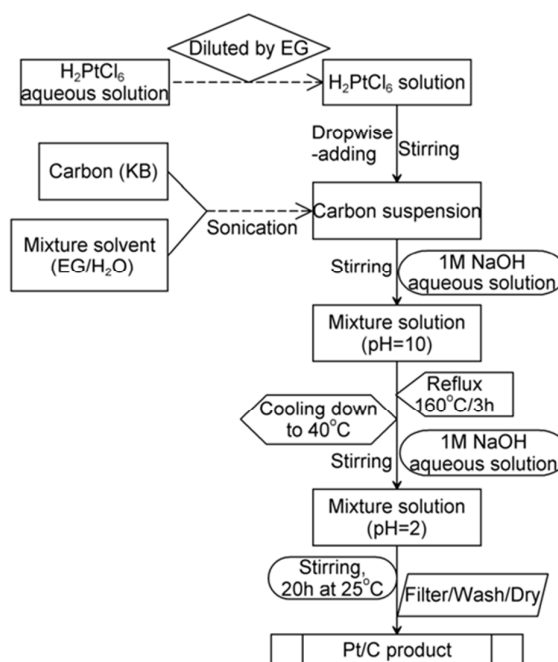


Fig. 1 Flowchart of the experimental preparation of a Pt/C catalyst.

Synthesis of Pt/C catalysts. The 50 wt% Pt/C catalysts were prepared by a modified polyol method using EG and water as a solvent mixture. A typical experimental procedure (See Figure 1) to synthesize the 50 wt% Pt/C catalysts is described as follows: a designated amount of carbon was added into a mixture containing different solvent ratios (25 ml of EG; 25 ml of EG/10 ml of H₂O; 25ml of EG/23 ml of H₂O; 25 ml of EG/28 ml of H₂O) in a 250 ml one-neck flask and sonicated for 1 h in an ultrasonic bath at room temperature to form a carbon suspension. In a beaker, a calculated amount of H₂PtCl₆ aqueous solution (22.16 wt%) was added into a 20 ml of EG. After sonicated for about 10 min, the H₂PtCl₆ solution was added drop-wise into carbon suspension in the flask under stirring. After 0.5 h, the pH of the mixture was slowly adjusted to 10 using a 1M NaOH aqueous solution. Subsequently, the

mixture was heated up to 160 °C under reflux and the temperature was kept for 3 h under stirring. Then, the mixture was rapidly cooled down to 40 °C and a 1M NaOH aqueous solution was used to adjust the pH to 2. Finally, the temperature was kept at 40 °C for 20 h under stirring. The mixture was filtered and washed using water until the pH of the filtrate reached around 7. The product was dried in a vacuum oven at 55 °C for 24 h to completely remove the solvent and subsequently was homogenized in a glass mortar. The used solvent ratios of EG to H₂O in the synthesis procedures are 45:0; 45:10; 45:23, and 45:28, respectively. The corresponding products are denoted as Pt/C(1), Pt/C(2), Pt/C(3), and Pt/C(4). The commercial carbon supported platinum catalyst was used as a compared catalyst that was labelled as Pt/TKK.

Physical characterization. X-ray diffraction (XRD) patterns of the catalysts were collected using a Bruker D8 Advanced X-ray diffractometer with Co-K α source ($\lambda=1.79021$ Å) in the 2θ range from 10° to 80°. The morphology and dispersion of Pt nanoparticles on carbon were examined using a traditional transmission electron microscope (TEM, Hitachi H7600). Thermogravimetric (TGA) measurements were performed on a thermal analyzer (TGA, Shimadzu TG-50H) in a temperature range of 25-800 °C with air flowing at 20 ml min⁻¹. Elemental analysis (EA) was conducted to test some elements such as carbon, hydrogen, and nitrogen for the catalysts. The interfacial chemistry and binding energy of the catalysts samples were investigated by X-ray photoelectron spectroscopy (XPS, Omicron & Leybold MAX200) using an Al K α source at 10 kV, 20 mA with the system pressure being 2×10^{-7} under the measurements. Binding energies were referenced to the Au 4f_{1/2} peak at 84.0 eV. The peak fitting of the XPS spectra was done with a Shirley function and Gaussian-Lorentzian function by the XPS PEAK 4.1 software.

Electrochemical characterization. Electrochemical studies were carried out at 25 °C in a standard three-electrode electrochemical cell using a rotating disk electrode (RDE) as the working electrode. A WaveDriver 10 potentiostat (Pine Research Instrumentation) was used to control the disk potentials and an AFMRX rotator (Pine Instrument) controlled the rotating speed. During the measurements, a Pt wire and a reversible hydrogen electrode (RHE) were employed as counter and reference electrodes, respectively, and 0.1 M HClO₄ was used as the electrolyte. All the potentials are versus RHE. The preparation of the working electrode was based on thin film method. Briefly, 10 mg of the catalyst sample was mixed with 9.5 ml of distilled water and 0.5 ml of iso-propyl alcohol under sonication for 1 h to make the catalyst ink; then 16 μ L of the ink was placed portion by portion onto a pre-cleaned glassy carbon (GC) electrode to form the catalyst layer; lastly, after solvent evaporation from the catalyst layer, 7 μ L of Nafion solution (5 wt%, Dupont) was dropped on top of the

disk to fix the catalyst layer on the GC surface. This coated electrode was then dried in air for 0.5 h. For electrochemical surface area measurements, cyclic voltammograms (CVs) (5 cycles at a scan rate of 20 mV s⁻¹ in the potential range of 0.03-1.2 V vs. RHE of the electrode) were recorded in a N₂-purged 0.1 M HClO₄ electrolyte. For ORR mass activity measurements, positive potential-going linear sweep voltammetry (LSV) was performed between 0.2 and 1.0 V vs. RHE at a potential scan rate of 5 mV s⁻¹ and an electrode rotation rate of 1600 rpm in an O₂-saturated 0.1 M HClO₄ electrolyte solution. For catalyst stability study, a standard cycling procedure were followed by running continuous potential cycling for 500 cycles between 0.6 and 1.2 V vs. RHE at a potential scan rate of 50 mV s⁻¹ in a N₂-purged 0.1 M HClO₄ electrolyte. After that, the I-V curves (5 cycles at a scan rate of 20 mV s⁻¹ in the potential range of 0.03-1.2 V vs. RHE of the electrode) were performed as the final electrochemical active surface areas (ECSA). Then, LSV between 0.2 and 1.0 V vs. RHE with a scan speed of 5 mV s⁻¹ at 1600 rpm was carried out in an O₂-saturated 0.1 M HClO₄ electrolyte solution to obtain the final ORR mass activity. In addition, accelerated durability tests (ADT) were also performed with 500 continuous potential cycling from 0.6 to 1.4 V for the best in-house catalyst and the Pt/TKK catalyst.

Results and Discussion

Figure 2 illustrates the XRD patterns of commercial Pt/TKK catalyst and various Pt/C catalysts synthesized in-house by different solvent ratios of EG/H₂O, and a typical XRD pattern for an unsupported Pt black (BASF) is given in Figure S1 (ESI). It can be observed in Figure S1 that two main characteristic peaks such as Pt(111) and Pt(200) located at 46.6° and 54.5°, respectively, in the scan range from 10° to 80°. From Figure 2, it is evidenced that all the carbon-supported Pt catalysts demonstrate two main characteristic peaks (i.e., Pt(111) and Pt(200)), which are in good agreement with those two peaks observed from the unsupported Pt black catalyst, indicating that the Pt precursor was successfully reduced in the modified polyol solution in which EG served as both a solvent and a reducing agent. During the Pt reduction, the Pt particle size increases with the Pt reduction reaction rate although the glycolate produced from EG oxidation can interact with Pt nanoparticles and hence act as a stabilizer.^{38,39} It was reported⁴¹ that the presence of H₂O, the concentration of EG could be reduced so that the reduction rate of Pt could be tuned during the polyol reduction, enabling the control of Pt size and distribution. As seen in Figure 2, with the addition of water in the synthesis, these two Pt peaks start to broaden and tend to appear within a low intensity, suggesting a decreasing Pt particle size. Among all of the Pt/C catalysts, the commercial Pt/TKK catalyst has two widest peaks characteristic of Pt. In addition, the diffraction peak at 28° is associated to carbon (002) plane, which also has a shift to a higher angle compared with that observed using Cu-K α as X-

ray source.⁴⁰ Based on the XRD patterns, the Pt crystallite sizes were calculated using the Deby-Scherrer equation⁴¹ and are presented in Table 1. It is found that the increase of EG/H₂O ratio does not monotonously influence the change of crystal size. At the EG/H₂O ratio of 45:23, the particle size of the self-

made Pt/C(3) catalyst is around 2.2 ± 0.5 nm, lower than those of other self-made Pt/C catalysts while showing comparable value to that of the commercial Pt/TKK catalyst.

The particle sizes of all the Pt/C catalysts were also obtained from the TEM images shown in Figure 3 and the derived size d-

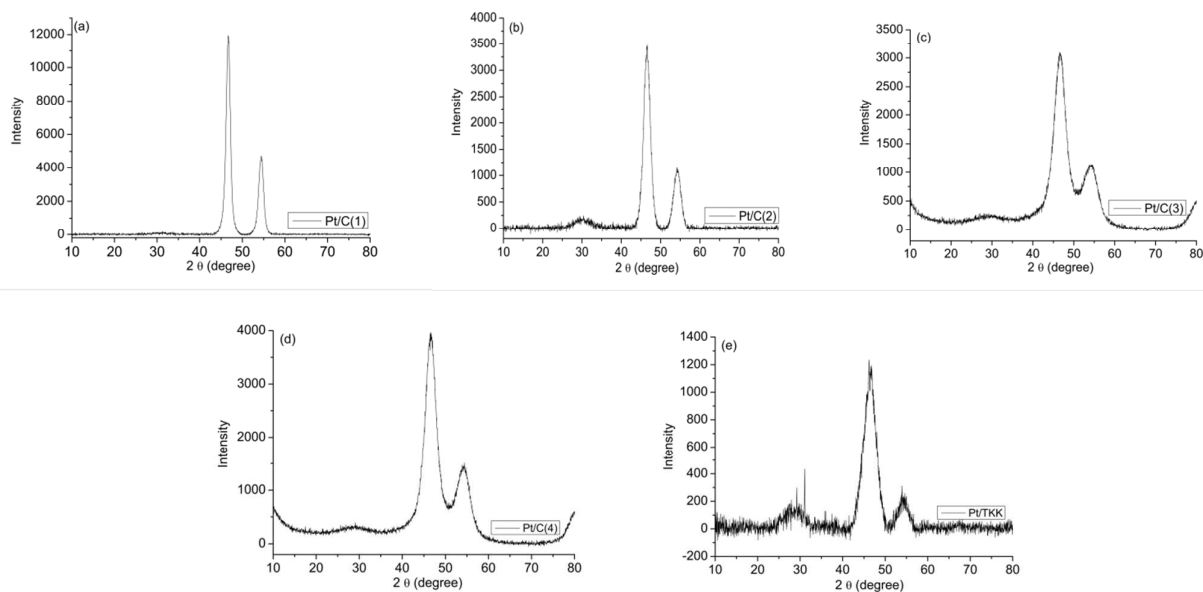


Fig. 2 X-ray diffraction patterns for various Pt/C catalysts: (a) Pt/C(1), (b) Pt/C(2), (c) Pt/C(3), (d) Pt/C(4), and (e) Pt/TKK.

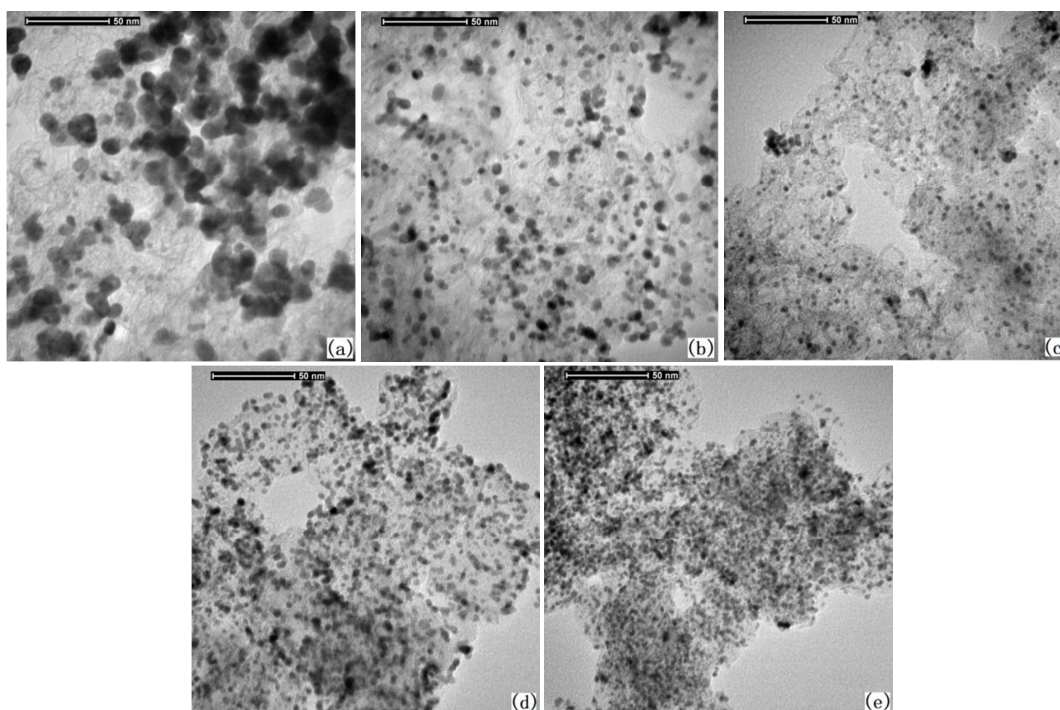
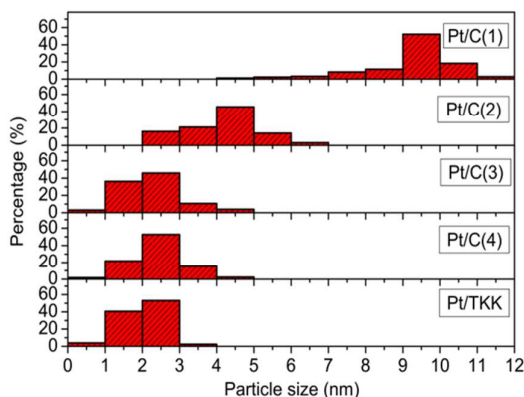
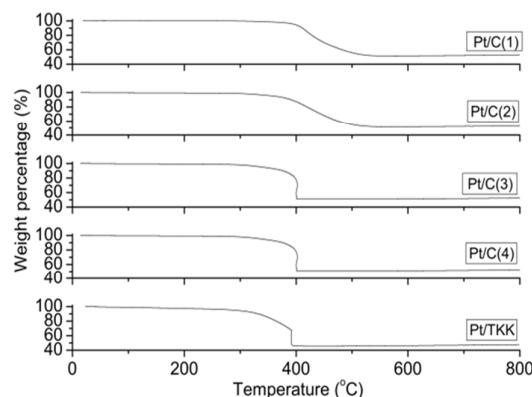


Fig. 3 TEM images of various Pt/C catalysts: (a) Pt/C(1), (b) Pt/C(2), (c) Pt/C(3), (d) Pt/C(4), and (e) Pt/TKK.

Table 1 Crystallite size and particle size of various Pt/C catalysts as a function of EG/H₂O ratio.

Sample	EG/H ₂ O ratio	Crystallite size, d_{XRD} (nm)	Particle size, d_{TEM} (nm)
Pt/C(1)	45:0	5.67	9.5 ± 0.5
Pt/C(2)	45:10	3.36	4.5 ± 0.5
Pt/C(3)	45:23	2.13	2.2 ± 0.5
Pt/C(4)	45:28	2.31	2.5 ± 0.5
Pt/TKK	-	2.03	2.1 ± 0.5

**Fig. 4** Particle size distribution of various Pt/C catalysts.**Fig. 5** TGA results for various Pt/C catalysts.

istribution is displayed in Figure 4. The numerical values of Pt particle sizes are also tabulated in Table 1 for comparison. Interestingly, the particle size are found to follow the same trend of the crystallite size although the particle size for a Pt/C catalyst obtained from TEM is a little bigger than the crystallite size derived from XRD due to a particle consisting of one or multiple crystal(s).

By examining the correlation between particle size and solvent ratio, it is seen that at first, the increasing proportion

Table 2 Composition of various Pt/C catalysts.

Sample type	Nominal composition			EA composition			TGA composition	
	Pt (wt%)	C (wt%)	Pt ^a (wt%)	C (wt%)	N (wt%)	H (wt%)	Pt ^b (wt%)	C ^b (wt%)
Pt/C(1)	50.00	50.00	51.75	48.25	0	0	51.45	48.55
Pt/C(2)	50.00	50.00	51.46	48.54	0	0	51.35	48.65
Pt/C(3)	50.00	50.00	51.54	48.46	0	0	51.05	48.95
Pt/C(4)	50.00	50.00	51.94	48.06	0	0	51.04	48.96
Pt/TKK	46.60	53.40	47.07	50.75	1.06	1.12	45.76	54.24

a: The percentage of Pt was calculated based on the tested contents of C, N, and H from EA results;

b: The percentages of Pt and carbon were calculated based on TGA results;

of water in the solvent mixture favours the reduction of particle size. However, after reaching a ratio of EG to H₂O of 45:23, the increasing proportion of water in the solvent mixture starts to result in increased particle sizes. The particle

size of the Pt/C(3) with the EG/H₂O ratio of 45:23 is the minimum (~2.2 ± 0.5 nm) among all catalysts, which is very close to that (~2.1 ± 0.5 nm) of the commercial Pt/TKK catalyst. In addition to the impact on particle size, the solvent ratio also a-

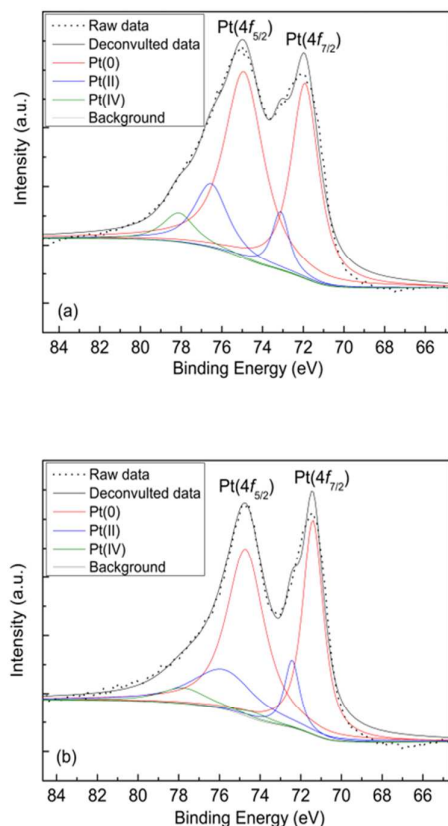


Fig. 6 XPS spectra for two Pt/C catalysts: (a) Pt/C(3) and (b) commercial Pt/TKK.

affects the size distribution and morphology of Pt particles. It can be observed from TEM images (Figure 3) that the use of pure EG in the synthesis demonstrates not only the highest particle size (9.5 ± 0.5 nm) but also a significant agglomeration of Pt particles. Moreover, with the addition of water in the solvent, particle size distribution becomes more homogenous and narrower, further indicating the positive impact of the addition of water into EG.

To examine the thermal property and confirm the composition of various Pt/C catalysts, TGA measurements were carried out from 25 to 800 °C. It can be found in Figure 5 that all of the curves show similar patterns representing similar thermal behaviour among various Pt/C catalysts but there are also subtle differences that might have some implications. Specifically, each curve starts to drop down from 300 °C, indicating the beginning of combustion of carbon; at around 400 °C, Pt/C(3) and Pt/C(4) exhibit the same sharp decline due to the complete combustion of carbon in their curves as the commercial Pt/TKK does while Pt/C(1) and Pt/C(2) have a slower decline in their curves. The slower decline in weight percentage of Pt/C(1) and Pt/C(2) catalysts may relate to the presence of residual EG that was not completely

removed during the synthesis process due to the high concentrations of EG used in the solvent mixture for Pt/C(1) and Pt/C(2). Based on the TGA results, elemental compositions of Pt and carbon were calculated for all catalysts and are presented in Table 2, together with the results from EA analysis. Clearly, the weight percentages of Pt and carbon obtained from TGA analysis are very close to the results from EA measurement. For all the Pt/C catalysts, the weight percentages of Pt and carbon from both of the TGA analysis and the EA measurement above have an experimental error in the range of 3%.

To further explore the effect of solvent ratio on the reduction of Pt precursor and the valence state of Pt nanoparticles in the self-made Pt/C catalysts, sample Pt/C(3) and the commercial Pt/TKK were analyzed by XPS. The XPS spectra in Figures 6 (a) and (b) show a strong doublet peak for both Pt/C(3) and Pt/TKK, representing a low energy band (Pt 4f_{7/2}) and a high energy band (Pt 4f_{5/2}). This suggests that the Pt species in the two carbon-supported Pt catalysts is present predominantly with zero-valence which has been reported to be the active site for electrochemical reaction.³¹ More importantly, Pt 4f_{7/2} can be found to be located at 72.12 eV for Pt/C(3) and at 71.43 eV for commercial Pt/TKK, respectively, indicating that the latter has more Pt oxides than the former. To further examine the oxidation states of the Pt, the relative presence of Pt(0), Pt(II), and Pt(IV) species was analyzed by Gaussian curve fitting of Pt 4f peaks.^{31,40} Based on the relative intensity, the percentages of Pt(0), Pt(II), and Pt(IV) are 72%, 18%, and 10%, respectively, for the Pt/C(3), and 71%, 22%, and 7%, respectively, for the commercial Pt/TKK, respectively. In the comparison of three valences of Pt species, the commercial Pt/TKK has a slightly higher percentage of Pt(II) than the Pt/C(3), suggesting a higher actual oxidation state in the Pt/TKK than that in the Pt/C(3), while the Pt/C(3) exhibits a little bit higher amount of Pt(IV) than the commercial Pt/TKK. From this result, the Pt(0) species has a high percentage (>70%) while the oxidized platinum species show a small percentage (<30%). Thus, for the Pt/C(3) and the commercial Pt/TKK, the Pt(0) surface should present the predominant active sites for electrochemical reaction rather than the Pt(II) and Pt(IV) species.⁴²

All electrochemical raw data are presented in Figure S2 (ESI) including CV and LSV tests for all catalysts. As shown in Figure S2 (ESI), all CV curves display a well-defined butterfly voltammetric feature of Pt in acid electrolytes in which a pair of broad voltammetric peaks in the potential range between +0.6 and +1.0 V result from the formation of Pt oxide in the anodic scan and the reduction of the Pt oxide in the return sweep. Two additional pair of voltammetric peaks are formed between 0 and +0.3 V because of hydrogen adsorption/desorption on the Pt surface. Based on the CV data, ECSAs for various self-made Pt/C catalysts were calculated using the integrated area of hydrogen adsorption/desorption

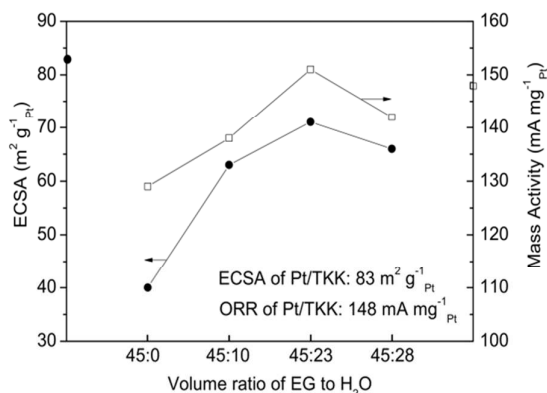


Fig. 7 Plots of ECSA values and Pt mass activities for various Pt/C catalysts as a function of the EG/H₂O ratio.

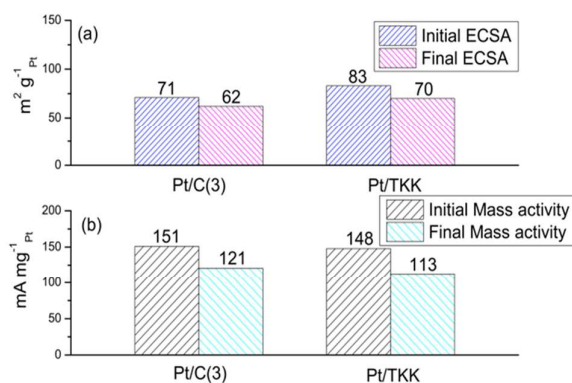


Fig. 8 (a) ECSAs and (b) ORR mass activities before and after 500 cycles of durability tests for Pt/C(3) and commercial Pt/TKK.

peaks⁴³⁻⁴⁵ and are presented in Figure 7. It can be observed that the ECSA of the self-made Pt/C increases with the addition of water in the solvent mixture, reaches the maximum value (ca. 71 m² g⁻¹Pt) at a EG/H₂O ratio of 45:23 and then starts to drop with a further increase of water. Interestingly, the trend of ECSAs of various catalysts matches the trend of Pt particle sizes in relation to EG/H₂O ratio with the turning point occurring both at the EG/H₂O ratio of 45:23, indicating a close relationship between Pt particle size and ECSA for Pt/C catalysts.

Based on the raw LSV data shown in Figure S2 (b and c), the mass activities of various catalysts for ORR were calculated at 0.9V using Koutecky-Levich theory^{46,47} and are plotted as a function of EG/H₂O ratio (also shown in Figure 7). Generally, the mass activity of the Pt/C catalyst for ORR is closely related to its ECSA⁴⁸, which is evidenced clearly in Figure 7. At the EG/H₂O ratio of 45:23, the mass activity of the self-made Pt/C

has a value of ca. 151 mA mg⁻¹Pt, which is comparable to that (ca. 148 mA mg⁻¹Pt) of the commercial Pt/TKK. In the experimental synthesis, the optimum control of the solvent ratio not only has positive impact on the structure and morphology of the catalyst particles, but also is favourable for the improved electrochemical properties of the Pt/C catalysts. The stability of the self-made Pt/C catalyst (Pt/C(3)) was first examined through cycling tests in the potential range of 0.6 to 1.0 V (vs RHE), and the same cycling tests were also performed with commercial Pt/TKK catalyst for comparison. Figure S3 presents the raw data of initial and final CV curves, and the initial and final LSV curves for both catalysts. Based on these raw data, the ECSA and ORR mass activity of the two catalysts before and after the cycling tests were calculated, and are compared in Figures 8 (a) and (b), respectively. For ECSA, the Pt/C(3) shows a decrease from 71 to 62 m² g⁻¹Pt with a loss of 13% that is slightly lower than the loss (ca. 16%) of the commercial Pt/TKK. For ORR mass activity, the Pt/C(3) also exhibits a smaller decrease from 151 to 121 mA mg⁻¹Pt (ca. 21%) than that of the commercial Pt/TKK catalyst (ca. 24%). To have a better insight into the durability of the catalysts, a harsher ADT test which subjects the catalysts to a potential cycling from 0.6 to 1.4 V, was also performed for both catalysts. As shown in Figure S4 (ESI), Pt/C(3) reveals an ECSA decrease of ca. 30% and a mass activity decrease of ca. 25%, which are also smaller than what observed for the Pt/TKK catalyst (i.e., a decrease of ca. 37% and 31% in ECSA and mass activity, respectively).

Conclusions

In this work, a series of 50 wt% Pt/C catalysts for ORR were fabricated using a simple modified polyol method in which various solvent volume ratios of EG/H₂O were controlled. The morphology, structure and electrochemical properties of these catalysts were investigated. The results of XRD and TEM indicated that the addition of water in solvent mixture played an important role in Pt particle size and size distribution. The TGA data confirmed the composition of Pt and carbon in the self-made Pt/C catalysts to be similar to the nominal one within an experimental error of 3%. The XPS spectra revealed that the self-made Pt/C had lower oxidation state than commercial Pt/TKK catalyst. Electrochemical measurement showed that, at the EG/H₂O ratio of 45:23, the self-made Pt/C exhibited a comparable electrocatalytic properties to those of commercial Pt/TKK, including ECSA, ORR mass activity and stability. It can be concluded that the addition of water into the EG solvent at a controlled ratio during the catalyst synthesis process promotes not only smaller particle sizes and more uniform size distribution but also favorable electrochemical characteristics of the catalyst in terms of mass activity and durability. These positive impacts have significant implications for applications in large scale production of Pt/C catalysts for PEM fuel cells, due to the simplicity of the synthesis process associated with the ease of filtering step when water is added into EG.

Acknowledgements

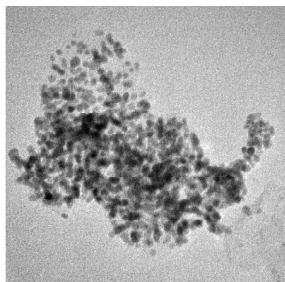
This work was supported by the Vancouver International CleanTech Research Institute Inc. (VICTRII) and a matching grant (452756-13) from Natural Sciences and Engineering Research Council of Canada Collaborative Research and Development (NSERC-CRD). The authors would also like to acknowledge the contribution of all members from Prof. Xiaotao Bi's catalyst group in the Department of Chemical and Biological Engineering at the University of British Columbia.

Notes and references

- B. Fang, M. Kim, S. Hwang and J.-S. Yu, *Carbon*, 2008, **46**, 876–883.
- G. Chai, B. Fang and J.-S. Yu, *Electrochem. Commun.*, 2008, **10**, 1801–1804.
- Y. –J. Wang, D. P. Wilkinson, V. Neburchilov, C. Song, A. Guest and J. Zhang, *J. Mater. Chem. A*, 2014, **2**, 12681–12685.
- J. H. Kim, B. Fang, S. B. Yoon and J.-S. Yu, *Appl. Catal. B: Environ.*, 2009, **88**, 368–375.
- Y. –J. Wang, D. P. Wilkinson, A. Guest, V. Neburchilov, R. Baker, F. Nan, G. A. Botton and J. Zhang, *J. Power Sources*, 2013, **221**, 232–241.
- Y. –J. Wang, D. P. Wilkinson and J. Zhang, *Dalton Trans.*, 2012, **41**, 1187–1194.
- B. Fang, J. H. Kim, C. Lee and J.-S. Yu, *J. Phys. Chem. C*, 2008, **112**, 639–645.
- B. Fang, J. H. Kim, M. Kim, M. Kim and J.-S. Yu, *Phys. Chem. Chem. Phys.*, 2009, **11**, 1380–1387.
- B. Fang, J. Kim, M. Kim and J. Yu, *Acc. Chem. Res.*, 2013, **46**, 397–1406.
- J. Kim, B. Fang, M. Song and J. Yu, *Chem. Mater.*, 2012, **24**, 2256–2264.
- J. H. Kim, B. Fang, M.-S. Kim, S. B. Yoon, T.-S. Bae, D. R. Ranade and J.-S. Yu, *Electrochim. Acta*, 2010, **55**, 7628–7633.
- B. Fang, J. Kim, M. Kim and J. Yu, *Chem. Mater.*, 2009, **21**, 789–796.
- J. Kim, B. Fang, M. Kim, V. Tricoli and J. Yu, *Catal. Today*, 2009, **146**, 25–30.
- M. Kim, B. Fang, N. Chaudhari, M. Song, T. Bae and J. Yu, *Electrochim. Acta*, 2010, **55**, 4543–4550.
- B. C. H. Steel and A. Heinzl, *Nature*, 2001, **414**, 345–352.
- K. Joon, *J. Power Sources*, 1998, **71**, 12–18.
- Y. –J. Wang, D. P. Wilkinson and J. Zhang, *Chem. Rev.*, 2011, **111**, 7625–7651.
- G. Cacciola, V. Antonucci and S. Freni, *J. Power Sources*, 2001, **100**, 67–79.
- K. Murata, *Electrochim. Acta*, 1995, **40**, 2177–2184.
- Y. Bing, H. Liu, L. Zhang, D. Ghosh and J. Zhang, *Chem. Soc. Rev.*, 2010, **39**, 2184–2202.
- X. Lin, L. Zheng, G. Gao, Y. Chi and G. Chen, *Anal. Chem.*, 2012, **84**, 7700–7707.
- Y. –J. Wang, N. Zhao, B. Fang, H. Li, X. Bi and H. Wang, *Chem. Rev.*, 2015, **115**, 3433–3467.
- B. Fang, N. K. Chaudhari, M.-S. Kim, J. H. Kim and J.-S. Yu, *J. Am. Chem. Soc.*, 2009, **131**, 15330–15338.
- B. Fang, M. S. Kim, J. H. Kim, M. Y. Song, Y. –J. Wang, H. Wang, D. P. Wilkinson and J.-S. Yu, *J. Mater. Chem.*, 2011, **21**, 8066–8073.
- M. K. Debe, *Nature*, 2012, **486**, 43–51.
- S. H. Hsieh, M. C. Hsu, W. L. Liu and W. J. Chen, *Appl. Surf. Sci.*, 2013, **277**, 223–230.
- C. –H. Pak, US Patent 7,132,385 B2.
- J. P. Owejan, J. E. Owejan and W. Gu, *J. Electrochem. Soc.*, 2013, **160**, F824–F833.
- A. Z. Weber, R. L. Borup, R. M. Darling, P. K. Das, T. J. Dursch, W. Gu, D. Harvey, A. Kusoglu, S. Litster, M. M. ench, R. Mukundan, J. P. Owejan, J. G. Pharoah, M. Secanell and I. V. Zenyuk, *J. Electrochem. Soc.*, 2014, **161**, F1254–F1299.
- J. M. Song, S. Y. Cha and W. M. Lee, *J. Power Sources*, 2001, **94**, 78–84.
- H.-Y. Park, D.-S. Yang, D. Bhattacharjya, M. Y. Song and J.-S. Yu, *Int. J. Hydrogen Energ.*, 2014, **39**, 1688–1697.
- E. Antolini, *Mater. Chem. Phys.*, 2003, **78**, 563–573.
- B. Le Gatié, H. Remita, G. Picq and M. O. Delcourt, *J. Catal.*, 1996, **164**, 36–43.
- S. Song, J. Liu, J. Shi, H. Liu, V. Maragou, Y. Wang and P. Tsiakaras, *Appl. Catal. B: Environ.*, 2011, **103**, 287–293.
- H. Liu, C. Song, L. Zhang, J. Zhang, H. Wang and D. P. Wilkinson, *J. Power Sources*, 2006, **155**, 95–110.
- S. Song, Y. Wang and P. K. Shen, *J. Power Sources*, 2007, **170**, 46–49.
- H.-Y. Park, D.-S. Yang, D. Bhattacharjya, M. Y. Song and J.-S. Yu, *Int. J. Hydrogen Energ.*, 2014, **39**, 1688–1697.
- J. M. Garcia-Gortes, J. Perez-Ramirez, M. J. Illan-Gomez and D. Salinas-Martinez de, *Catal. Commun.*, 2003, **4**, 165–170.
- H. –S. Oh, J. –G. Oh, Y. –G. Hong, H. Kim, *Electrochim. Acta* 2007, **52**, 7278–7285.
- W.-D. Lee, D.-H. Lim, H.-J. Chun and H.-I. Lee, *Int. J. Hydrogen Energ.*, 2012, **37**, 12629–12638.
- A. L. Patterson, *Phys. Rev.*, 1939, **56**, 978–982.
- P.-L. Kuo, W.-F. Chen, H. Y. Hhang, I. –C. Chang and S. A. Dia, *J. Phys. Chem. B*, 2006, **110**, 3071–3077.
- G. He, Y. Song, K. Liu, A. Walter, S. Chen and S. Chen, *ACS Catal.*, 2013, **3**, 831–838.
- A. Pozio, M. Francesco, A. Cemmi, F. Cardellini and L. Giorgi, *J. Power Sources*, 2002, **105**, 13–19.
- F. –Y. Xie, Z. –Q. Tian, H. Meng and P.-K. Shen, *J. Power Sources*, 2005, **141**, 211–215.
- A. J. Bard and L. R. Faulkner, *Electrochemical Methods: Fundamentals and Applications*, second ed., John Wiley & Sons, New York, NY, 2001, 196.
- E. Higuchi, H. Uchida and M. Watanabe, *J. Electroanal. Chem.*, 2005, **583**, 69–76.
- W. Zhang, J. Chen, G. F. Swiegers, Z. –F. Ma and G. G. Wallace, *Nanoscale*, 2010, **2**, 282–286.

Table of Contents (TOC)

1. Color graphic (maximum size 8cm × 4cm):



2. Text (one sentence, of maximum 20 words, highlighting the novelty of the work)

“Particle size and distribution of 50 wt% Pt/C can be determined by the volume ratio of EG/H₂O in the synthesis”.